

Article

# Study of $^{222}\text{Rn}$ – $^{220}\text{Rn}$ Measurement Systems Based on Electrostatic Collection by Using Geant4+COMSOL Simulation

Luigi Rinaldi <sup>1</sup>, Fabrizio Ambrosino <sup>1,2</sup>, Vincenzo Roca <sup>3</sup>, Antonio D'Onofrio <sup>1,3</sup> and Carlo Sabbarese <sup>1,3,\*</sup>

<sup>1</sup> Department of Mathematics and Physics, University of Campania “L. Vanvitelli”, Viale Lincoln 5, 81100 Caserta, Italy; 1995luigirinaldi@gmail.com (L.R.); fabrizio.ambrosino@unina.it (F.A.); antonio.donofrio@unicampania.it (A.D.)

<sup>2</sup> Department of Agricultural Sciences, University of Naples “Federico II”, Portici, Italy

<sup>3</sup> National Institute of Nuclear Physics, Via Cinthia 21, 80126 Napoli, Italy; vroca222@gmail.com

\* Correspondence: carlo.sabbarese@unicampania.it

**Abstract:** Using Monte Carlo (with Geant4) and COMSOL simulations, the authors have defined a useful tool to reproduce the alpha spectroscopy of  $^{222}\text{Rn}$ ,  $^{220}\text{Rn}$  and their ionized daughters by measurement systems based on electrostatic collection on a silicon detector, inside a metallic chamber. Several applications have been performed: (i) simulating commercial devices worldwide used, and comparing them with experimental theoretical results; (ii) studying of realization of new measurement systems through investigation of the detection efficiency versus different chamber geometries. New considerations and steps forward have been drawn. The present work is a novelty in the literature concerning this research framework.

**Keywords:** radon detector; electrostatic collection; Monte Carlo simulation; Geant4; COMSOL; detection efficiency



**Citation:** Rinaldi, L.; Ambrosino, F.; Roca, V.; D'Onofrio, A.; Sabbarese, C. Study of  $^{222}\text{Rn}$ – $^{220}\text{Rn}$  Measurement Systems Based on Electrostatic Collection by Using Geant4+COMSOL Simulation. *Appl. Sci.* **2022**, *12*, 507. <https://doi.org/10.3390/app12010507>

Academic Editor: Francesco Caridi

Received: 21 October 2021

Accepted: 1 January 2022

Published: 5 January 2022

**Publisher's Note:** MDPI stays neutral with regard to jurisdictional claims in published maps and institutional affiliations.



**Copyright:** © 2022 by the authors. Licensee MDPI, Basel, Switzerland. This article is an open access article distributed under the terms and conditions of the Creative Commons Attribution (CC BY) license (<https://creativecommons.org/licenses/by/4.0/>).

## 1. Introduction

Radon (Rn) is a natural radioactive gas present in the environment. Two are the main isotopes:  $^{222}\text{Rn}$  (radon) with a decay half-life of 3.823 days, and  $^{220}\text{Rn}$  (thoron) with a half-life of 55.8 s. Both are carefully studied worldwide by the scientific community especially for radioprotection purposes [1,2] and for geophysical phenomena tracking [3,4]. These goals require measurement systems suitable for monitoring the gas isotopes. Various methods for Rn detection have been developed throughout the years, those based on solid-state nuclear track detection and electrostatic collection are the most widespread and used nowadays [5]. The first method utilizes plastic devices sensitive to  $\alpha$ -radiation emitted by Rn and decay products, for mean long-term monitoring [6]. In the second method, naturally ionized Rn daughter, inside a metallic chamber put to a high voltage, are electrostatically driven on to the surface of a silicon detector set to ground potential, enabling the collection of full alpha energies and obtaining high resolution  $\alpha$ -spectrometry. The electrostatic collection systems have optimal detection efficiencies; they allow the continuous detection of the Rn by distinguishing both gas isotopes with their progeny [7]. Currently, three are the main commercial devices for measuring environmental Rn concentrations based on electrostatic collection (by diffusion or pumping the gas in the detection chamber): RAD7 (Durrige Company, Billerica, MA, USA) [8]; RaMonA (University of Naples and University of Campania-Caserta, Italy) [9]; Radim3A (Tesla Company, Pruhonice, Czech Republic) [10]. Rn measurements and the development of new detection systems remain popular topics [11]. Using of tools for the simulation is a required and useful part for the complete evaluation and realization of such kind of Rn measurement systems. In particular, it is necessary to reproduce the geometry of the system, and simulate the  $\alpha$ -spectrum of the Rn with progeny and the correspondent detection efficiency for each involved radionuclides. This leads to being able to study the efficiency versus the different geometries of the system,

in order to find the best experimental solution to be realized. Different Rn measurement systems can, hence, be developed for several purposes. Tools for the simulation of the particles passage through matter are based on Monte Carlo method, the major ones are FLUKA and Geant4 [12]. Both can handle complex 3D-geometries using combinatorial geometry algorithms.

In literature, papers focused on Rn monitoring only use commercial devices for their purposes, without worrying about simulations [13,14]; while papers focused on investigation of new Rn measurement systems only deal with the realization and the testing of them without handling the simulation [15–17]. Within the research framework of simulation of Rn detection systems, in particular those based on electrostatic collection, very few studies are published, e.g., a low-cost monitor for the thoron [18,19] and radon [20] measurement was designed. These studies obtained results by using FLUKA or Geant4 with restrictions due to the gaps of both simulation tools. In [19] only non-ionized  $^{220}\text{Rn}$  atoms are simulated with FLUKA, while in [18,20] the efficiency of  $^{220}\text{Rn}$  and the spatial distribution of  $^{214}\text{Po}$  ions were determined using Geant4 with a constant electric field inside the metallic chamber. In fact, FLUKA does not allow to add the electric field, contrary to Geant4 where it is possible but constant or as a function of spatial coordinates. For these reasons, in the present work we introduce the COMSOL software, a powerful tool for the resolution of problems at partial differential equations, which simulates an electric field as gradient of the applied potential difference within metallic chamber and creates the correspondent map useful for Geant4 input [21]. The aim of our work is to provide a useful and standard methodology for the study of radon and thoron measurement systems based on electrostatic collection by using Geant4+COMSOL simulation tools. The main commercial devices will be simulated and the results compared with the experimental ones. Due to the short  $^{220}\text{Rn}$  half-life, in works [18,19] emerge the importance of the realization of systems for the direct detection of the  $\alpha$ -particles produced by the non-ionized  $^{220}\text{Rn}$  atoms, to avoid their energy loss before they reach the detector. Therefore, a simulation study of the detection efficiency of  $^{222-220}\text{Rn}$  and their progeny versus different geometries of measurements system is also performed.

## 2. Software

Geant4 (Geometry and Tracking, 4th generation) is the used software for the simulation of the electrostatic detection of  $^{222-220}\text{Rn}$  and their progeny on a silicon detector inside a high voltage metallic chamber. Geant4, a publicly available Monte Carlo toolkit developed at CERN, is used to perform accurate simulations of the interaction and transport of particles through matter [22]. Its fields of application include high energy, nuclear and accelerator physics, as well as studies in medical and space science. Unlike the other computational Monte Carlo codes, such as FLUKA, Geant4 is not an executable program but rather a set of C++ class libraries for running, tracking, stepping and collecting information. The version 10.7 of Geant4 for Windows platform, released in December 2020, has been used in this work. COMSOL Multiphysics (or simply COMSOL) is used to simulate the electric field generated within the metallic chamber walls of the Rn measurement system for the electrostatic collection of the gas isotopes daughters. COMSOL is a finite element analysis and free solver software package for various physics and engineering applications [21]. It includes an environment for modeling any physical phenomenon that can be described using ordinary (ODEs) or partial differential equations (PDEs). Electrostatic module of COMSOL has been used to determine the values of the electric fields, as potential gradient, to be used in Geant4. COMSOL version 5.5 for Windows platform, released in February 2020, has been used in this work. Geant4 provides several widget toolkits for creating graphical user interfaces and visualization system of results. Qt application has been chosen being fast, smart and open-source. Moreover, a Matlab code has been developed and used to plot the spectrum data obtained with Geant4+COMSOL simulation and for the statistical analysis of the results.

### 3. Methods and Simulation

#### 3.1. Decay Process and Electrostatic Collection

$^{222}\text{Rn}$  and  $^{220}\text{Rn}$  decay by emitting  $\alpha$ -particles with energy of 5.49 MeV and 6.30 MeV respectively.  $^{222}\text{Rn}$   $\alpha$ -emitter daughters are  $^{218}\text{Po}$  (6.02 MeV) and  $^{214}\text{Po}$  (7.68 MeV); while those of  $^{220}\text{Rn}$  are  $^{216}\text{Po}$  (6.77 MeV),  $^{212}\text{Bi}$  (6.09 MeV) and  $^{212}\text{Po}$  (8.77 MeV). The  $\alpha$ -particles in air lose some or all of their energy before to hit the detector, except those emitted nearby that can be detected with full energy [23]. It is well known that the daughter nuclei of  $^{222}\text{Rn}$  and  $^{220}\text{Rn}$  become positively charged in air: at atmospheric pressure and temperature, with a standard relative humidity of 45%, the fraction of ionized daughters of radon e thoron is 88%, the remaining 12% are neutral [24]. Therefore, it is possible to electrostatically collect the 88% part that will decay with full  $\alpha$ -energy on detector, inside a metallic chamber. To achieve the electrostatic collection, a high potential difference is applied between chamber and detector: an electric field is formed inside the detection chamber and the positive charged ions can be collected on the detector surface grounded. Instead,  $^{222}\text{Rn}$ ,  $^{220}\text{Rn}$  and about their 12% daughters are neutrally charged in air; a direct detection of them is possible and the emitted  $\alpha$ -particles arrive with energy depending on the sizes of the chamber [18,24].

From the simulation point of view, to reproduce the physical process above described in Geant4, the pre-package physics list *QGSP\_BERT\_HP*, recommended for low energy dosimetric application, is used, which contains the process *G4RadioactiveDecay* to simulate radioactive decay processes. The radionuclides production is made by *G4VUserPrimaryGeneratorAction* class, where through the use of the *GeneratePrimaries()* method they are defined by specifying the atomic number, mass number, ion charge and excitation energy. Each radionuclide is simulated separately, distinguishing between ionized and non-ionized and respecting the percentage proportions of the decay chain to which it belongs. For our purposes,  $^{222-220}\text{Rn}$  and their progeny are generated randomly with a uniform probability density function (PDF) within the whole chamber volume. This is performed with the random number generator by *G4UniformRand()*. Emitted  $\alpha$ -particles produced during decay are generated by choosing a random emission direction in the whole  $4\pi$  solid angle.

#### 3.2. Geometry of Measurement System and $\alpha$ -Detector

The measurement system consists of a silicon detector that is an active element and a metallic chamber, of with different shapes and dimensions, in which the detector is mounted. Since high voltage is applied to the chamber walls, the detector and the chamber are electrically isolated by means of a thin polyethylene layer wrapping the detector non active surfaces [20]. Silicon detectors are known to trap  $\alpha$ -radiation and to measure the effect of incident charged particles. They provide high-resolution; the electrostatic transport allows high-efficiency alpha spectroscopy and very low background.

From the simulation point of view, to design the system geometry and define the materials in Geant4, the *Construct()* method is used by the *G4RunManager* class. Materials, the 'world' environment and all components must be defined. Firstly, the creation of the 'world' environment is required as physical volume that represents the experimental area and contains all other components. Inside the 'world', the shape of the system with the detector can be defined, by *G4VSolid* class. This class has several preset shapes already implemented, such as parallelepiped, hemisphere and cylinder with *G4Box*, *G4Sphere* and *G4Tubs* respectively. The volume inside the system, where the investigated radionuclides move, is filled by air. The *G4Material Data-Base* allows choosing the material to be assigned to the system components. The silicon detector uses *G4\_Si* material; the air volume uses *G4\_AIR*, which is surrounded by a metal grid made of *G4\_Fe* material. The insulator, made up by *G4\_POLYETHYLENE*, is placed between detector and metal grid. The 3D-coordinates of the system within the 'world' are defined by *G4VPhysicalVolume*. The silicon detector is made sensitive to  $\alpha$ -radiation by *SensitiveDetector+HitsCollection* tools.

### 3.3. Calculation of the Electric Field with COMSOL

In order to electrostatically drive the  $^{222-220}\text{Rn}$  progeny ions on the silicon detector, a specific high voltage ( $V$ ) is applied to the metallic walls of the chamber to generate an electric field ( $\vec{E}$ ) between them and the detector surface, according to the following PDEs:

$$\vec{E} = -\vec{\nabla}V \quad (1)$$

$$\vec{\nabla} \cdot (\epsilon_0 \epsilon_r \vec{E}) = \rho \text{ [Gauss's law]} \quad (2)$$

where  $\epsilon_0$  and  $\epsilon_r$  are respectively the dielectric constants in vacuum and relative to the material, and  $\rho$  is the volume charge density [25]. In our case, high voltage equipment, space charges due to ions are negligible ( $\rho = 0$ ) and therefore the equation to be solved for the dielectric media is:

$$\vec{\nabla} \cdot [\epsilon_0 \epsilon_r (-\vec{\nabla}V)] = 0. \quad (3)$$

The program solves (3) for voltage (potential) distribution  $V$  over user defined domain with sources and boundary condition.

From the simulation point of view, in COMSOL it is necessary to reproduce the same geometry and materials of the measurement system defined in Geant4, so that the dimensions coincide. This is essential in order to avoid code errors of the interaction between the two simulation tools. The COMSOL panel control is well organized and particularly intuitive: with the 'Model Tree' command it is possible to edit each step of the whole simulation process, i.e., defining 3D-geometry and materials of the system, specifying the PDEs that describe the physical phenomenon, solving the PDEs and then obtaining the solutions. By using *Geometry Tool* of 'Model Tree' command it is possible to introduce several geometrical shapes (such as blocks, cones, cylinders, spheres) for the realization of the system components. The materials of the objects previously created is performed using the *Material Library* provided by the software. A defined high voltage is applied to the metallic walls of the chamber, and the optimal bias voltage (to ground) is applied to the detector (25 V). The involved PDEs, above described, for the generation of the electric field are selected by *Electric Potential Tool*. Then, it is possible to start the simulation by *Run* command. The data that the user can save and plot are stored in the *Results* section of the software. COMSOL simulates the flow rate of air sampling assembly, electric field map and particle trajectories in the 3D-geometry. Using the *3D Plot Group*, the simulated potential distribution and the electric field spatial distribution can be obtained respectively. The electric field map, to be used in Geant4, is exported to a text-file by using the command *Copy Plot Data to Clipboard*. The field map contains the coordinates and the value of the electric field in the chamber volume.

### 3.4. Simulation and Spectrum Formation

Once the electric field map is created (Section 3.3) and fed to Geant4 simulation (Sections 3.1 and 3.2), it is possible to launch the application by using */run/beamOn* command with  $10^8$  primary starting particles source (enough to make small the error). The developed simulation is time-independent; this means: (i) Rn diffusion processes in the system are not taken into account and, hence, each radionuclide is originated in the whole volume; (ii) the equilibrium between parent and daughter radionuclides is assumed (after  $\sim 4$  h for  $^{222}\text{Rn}$ , and after  $\sim 4$  days for  $^{220}\text{Rn}$ ). The simulation results are used to generate an energy spectrum. The *G4AnalysisManager* class is used to create and fill a 1D-histogram (the spectrum) of the energy deposited per event for sensitive detector volume.

These data are stored in a CSV-file for each individual radionuclide; then, they are combined together into a single file using specially developed Matlab code.

## 4. Results and Discussion

Worldwide-used commercial devices for Rn detection, based on electrostatic collection, have been simulated with our developed procedure by using Geant4+COMSOL. The results

will be compared with the experimental ones provided in literature and/or stated by the manufacturer company. The simulated devices are:

- RAD7 (Durrige Company, USA), likely the most known and used, consisting of a hollow hemispherical metallic chamber of  $700 \pm 5 \text{ cm}^3$  volume, with a silicon surface barrier detector, having a  $300 \pm 1 \text{ mm}^2$  circular active area, centered on the bottom [26].
- RaMonA (University of Naples and University of Campania-Caserta, Italy), consisting of a  $785 \pm 8 \text{ cm}^3$  hollow cylindrical metallic chamber,  $10.0 \pm 0.1 \text{ cm}$  high and  $10.0 \pm 0.1 \text{ cm}$  diameter, with a silicon surface barrier detector, having a  $50.0 \pm 0.4 \text{ mm}^2$  circular active area, centered on the top [27].
- Radim3A (Tesla company, Czech Republic), consisting of a hollow hemispherical metallic chamber of  $830 \pm 5 \text{ cm}^3$  volume, and a silicon surface barrier detector, having a  $450 \pm 2 \text{ mm}^2$  circular active area, centered 1 cm below on the bottom [10].

The sampling of the measuring air takes place by diffusion of  $^{222-220}\text{Rn}$  inside the chamber in Radim3A; inside RaMonA the air is pumped; while RAD7 works in both ways. The high voltage power circuit of the three systems charges the metallic chamber to a potential of 2500 V for RAD7, 2000 V for Radim3A, and 3500 V for RaMonA, creating an electric field throughout the volume that propels  $^{222-220}\text{Rn}$  positively charged particles onto the detector [8–10].

In all systems, the detector is insulated in a plastic holder. The systems have an experimentally estimated detection efficiency of  $^{218}\text{Po}$  (about the same assumed for  $^{216}\text{Po}$  [23]) of:  $0.007 \pm 0.001 \text{ cpm} \cdot \text{m}^3 \cdot \text{Bq}^{-1}$  ( $0.11 \pm 0.03 \text{ cps} \cdot \text{L} \cdot \text{Bq}^{-1}$ ) for RAD7,  $0.8 \pm 0.1 \text{ count} \cdot \text{m}^3 \cdot \text{Bq}^{-1} \cdot \text{h}^{-1}$  ( $0.22 \pm 0.02 \text{ cps} \cdot \text{L} \cdot \text{Bq}^{-1}$ ) for Radim3A, and  $0.047 \pm 0.005 \text{ cps} \cdot \text{L} \cdot \text{Bq}^{-1}$  for RaMonA [26,27]. Considering the volume of the three chambers, the systems have  $^{218-216}\text{Po}$  detection efficiency of:  $16 \pm 4\%$  for RAD7,  $27 \pm 3\%$  for Radim3A, and  $6 \pm 1\%$  for RaMonA.

Geant4+COMSOL simulation reproduce the geometries of the three investigated measurement systems, with the specific features of the electric field generated inside the chamber. The thicknesses of the metallic chamber, the detector insulator holder and the detector sensitive surface are set at 1 mm, 2 mm and  $500 \mu\text{m}$ , respectively (not affecting the simulation). In Figure 1 are reported the 3D-model geometry of the three Rn measurement systems in Geant4, together with the correspondent simulated electric potential spatial distributions and electric field flow lines inside the metallic chamber by COMSOL.

An example of spectrum of mixed atmospheres of  $^{222}\text{Rn} + ^{220}\text{Rn}$  from Geant4+COMSOL simulation in the RaMonA device is reported in Figure 2, compared with an experimental one [23,28].

The simulated efficiency, obtained by the spectrum from Geant4+COMSOL, is computed as the ratio between the alpha particles detected on the Silicon detector and the number of alpha primary starting particles generated in the detection volume of chamber. The efficiency uncertainty comes from the propagation error of both elements of the ratio [19], where the numerator error is the square root of the counts sum. The efficiencies of the three measurement systems obtained by Geant4+COMSOL are the following:  $16 \pm 2\%$  for RAD7,  $5 \pm 2\%$  for RaMonA, and  $28 \pm 3\%$  for Radim3A. These results are perfectly consistent, considering the uncertainties, with the experimental ones provided in literature and/or stated by the manufacturer, which are  $16 \pm 4\%$  for RAD7,  $6 \pm 1\%$  for RaMonA, and  $27 \pm 3\%$  for Radim3A.

A further study has been performed to simulate, by Geant4+COMSOL, two different versions of RaMonA system, called Ramonino and Ramonello, used in diffusion mode respectively as the reference monitor in the Rn exposure facility of Universities of Naples and Campania, and referred to the ENEA (National Metrology Institute of Ionizing Radiation Metrology in Italy) respectively [29–33]. Ramonino and Ramonello consist of  $190 \pm 4 \text{ cm}^3$  and  $300 \pm 5 \text{ cm}^3$  hollow hemispherical metallic chambers with silicon surface barrier detectors, having a  $50.0 \pm 0.4 \text{ mm}^2$  and  $100 \pm 1 \text{ mm}^2$  circular active area, on the bottom, respectively [28]. The basis of the hemispherical chamber of both systems has a hole for the detector (insulated in a plastic holder). A high voltage of 1500 V is applied to the metallic chamber of both systems, to electrostatically collect  $^{222-220}\text{Rn}$  ionized daughters

on the detector. Experimentally, the measurement systems have a  $^{218-216}\text{Po}$  detection efficiency of:  $0.0108 \pm 0.0003 \text{ cps}\cdot\text{L}\cdot\text{Bq}^{-1}$  for Ramonino, and  $0.0275 \pm 0.0008 \text{ cps}\cdot\text{L}\cdot\text{Bq}^{-1}$  for Ramonello [28]. Considering the volume of the two measurement chambers, Ramonino and Ramonello have  $6.0 \pm 0.2\%$  and  $9.0 \pm 0.3\%$  of  $^{218-216}\text{Po}$  detection efficiencies. In addition, in this case, the simulated efficiencies of Ramonino and Ramonello, i.e.,  $6 \pm 1\%$  and  $8 \pm 2\%$ , by Geant4+COMSOL agree within uncertainty with the experimental ones. No figures of the Ramonino and Ramonello systems are shown because they are in [28] and, also, have geometries similar to those of RAD7 and Radim3A and, therefore, from the simulation point of view they would have been similar and brought only an overload of repetitive figures.

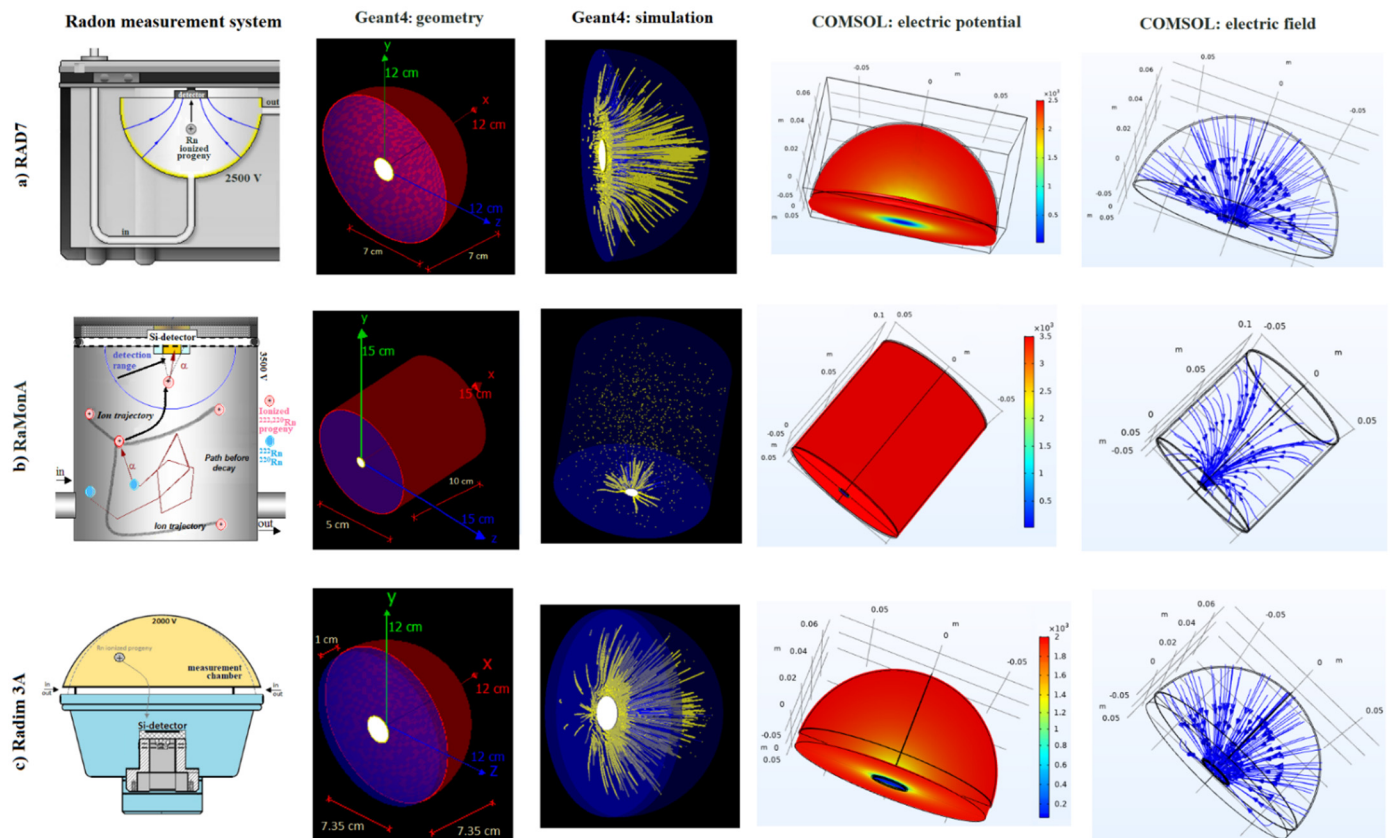


**Figure 1.** Schematic view of the Geant4 and COMSOL simulations of the three main worldwide commercial  $^{222-220}\text{Rn}$  measurement system RAD7 (a), RaMonA (b) and Radim3A (c). For Geant4 are shown the 3D geometry and simulation of the primary starting particles source; for COMSOL are shown the simulated electric potential spatial distributions and electric field flow lines.

Based on all previous considerations, a new Rn monitoring device (Ramonetto) has been designed and realized to be used in diffusion mode as new improved reference monitor in the Rn exposure facility of Universities of Naples and Campania. It consists of a  $1072 \pm 3 \text{ cm}^3$  hollow hemispherical metallic mesh chamber with a silicon PIN photodiode detector, having a  $784 \pm 2 \text{ mm}^2$  square active area, on the bottom (insulated in a plastic holder). A voltage of 2500 V is applied to the metallic chamber to electrostatically collect  $^{222-220}\text{Rn}$  ionized daughters on the detector. The measurement system has a high  $^{218-216}\text{Po}$  detection efficiency of:  $0.25 \pm 0.03 \text{ cps}\cdot\text{L}\cdot\text{Bq}^{-1}$ , and  $24 \pm 3\%$  considering the volume of the measurement chamber. Again, the efficiency of the new device is consistent with the simulated one of  $23 \pm 4\%$  by Geant4+COMSOL. The experimental efficiency of Ramonino, Ramonello and Ramonetto were obtained using  $^{222}\text{Rn} + ^{220}\text{Rn}$  mixed atmospheres realized by calibrated sources of a pylon RNC-RN-1025  $^{226}\text{Ra}$  for  $^{222}\text{Rn}$ , and  $^{232}\text{Th}$  salts for  $^{220}\text{Rn}$  [28]. Figure 3a shows Ramonetto measurement system. It is worth mentioning that to choose

the right high voltage value to be applied to the chamber walls of Ramonetto, experimental and simulated tests have been carried out on the  $^{218}\text{Po}$  counts per seconds (cps) versus the applied voltage value. As seen in Figure 3(a.1), the value of 2500 V has been chosen since the maximum cps saturation is reached. As Ramonetto geometry shape is equal to those of RAD7/Radim3A, no figures of Geant4 and COMSOL are shown being the simulations similar.

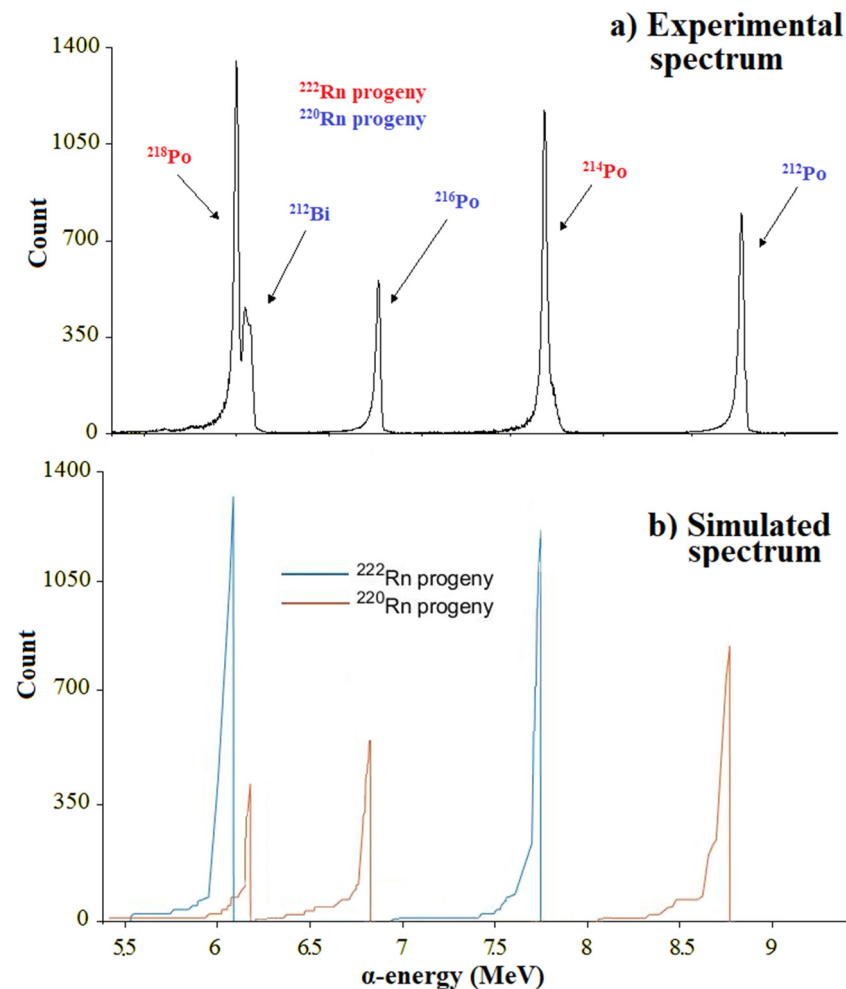


**Figure 2.** Experimental (a) and Geant4+COMSOL simulated (b) spectrum of  $^{222}\text{Rn}$  ( $6344 \pm 541$  Bq) +  $^{220}\text{Rn}$  ( $3258 \pm 356$  Bq) mixed atmospheres in the RaMonA measurement system [23].

Referring to the work [18] that presents a new reference measurement system (Sabot chamber) mainly focused on the  $^{220}\text{Rn}$  (and also its ionized progeny) direct detection by diffusion, small enough to reduce as much as possible the energy loss of the non-ionized  $^{220}\text{Rn}$  alpha particles before they reach the detector (due to  $^{220}\text{Rn}$  short half-life of 55.8 s), we reproduced experimentally and by simulation that chamber. The Sabot chamber is a 1 cm high metallic chamber with a surface composed of a silicon detector of diameter 4 cm: the active volume is  $13.0 \pm 0.1$  cm<sup>3</sup>. With 1000 V potential applied to the chamber, the  $^{220}\text{Rn}$  efficiency value is  $35 \pm 2\%$ , by using a Pylon  $^{228}\text{Th}$  source to create a  $^{220}\text{Rn}$  atmosphere [18]. We have made a similar chamber (RadonSmall, Figure 3b) using a hollow parallelepiped metallic mesh chamber, having a volume of  $7840 \pm 8$  mm<sup>3</sup>. A silicon PIN photodiode detector, having a square active area of  $784 \pm 2$  mm<sup>2</sup> and insulated in a plastic holder, acts as a basis. By using  $^{220}\text{Rn}$  atmosphere realized with a calibrated source of  $^{232}\text{Th}$  salts, and by applying a voltage of 200 V on the metallic walls of the chamber, the  $^{220}\text{Rn}$  detection efficiency is  $24 \pm 2\%$ . In addition, for RadonSmall, to choose the best voltage value to be applied to the chamber walls, experimental and simulated tests have been carried out on the  $^{216}\text{Po}$  counts per second (cps) as the applied voltage varied, to reach the maximum

cps saturation. The  $^{220}\text{Rn}$  efficiency by Geant4+COMSOL simulations (Figure 3(b.1)) gives the values of  $23 \pm 4\%$ , in agreement with the experimental one. It is important to point out that in Sabot chamber and in RadonSmall, the non-ionized  $\alpha$ -particles peak of  $^{220}\text{Rn}$  is obtained with the procedure described in [18,19]: subtracting from the total spectrum ( $^{220}\text{Rn} + ^{216}\text{Po} + ^{212}\text{Bi} + ^{212}\text{Po}$ ) the spectrum collected after eliminating the  $^{220}\text{Rn}$  and consisting of  $^{212}\text{Bi} + ^{212}\text{Po}$  that is achieved simply by removing the  $^{228-232}\text{Th}$  source.

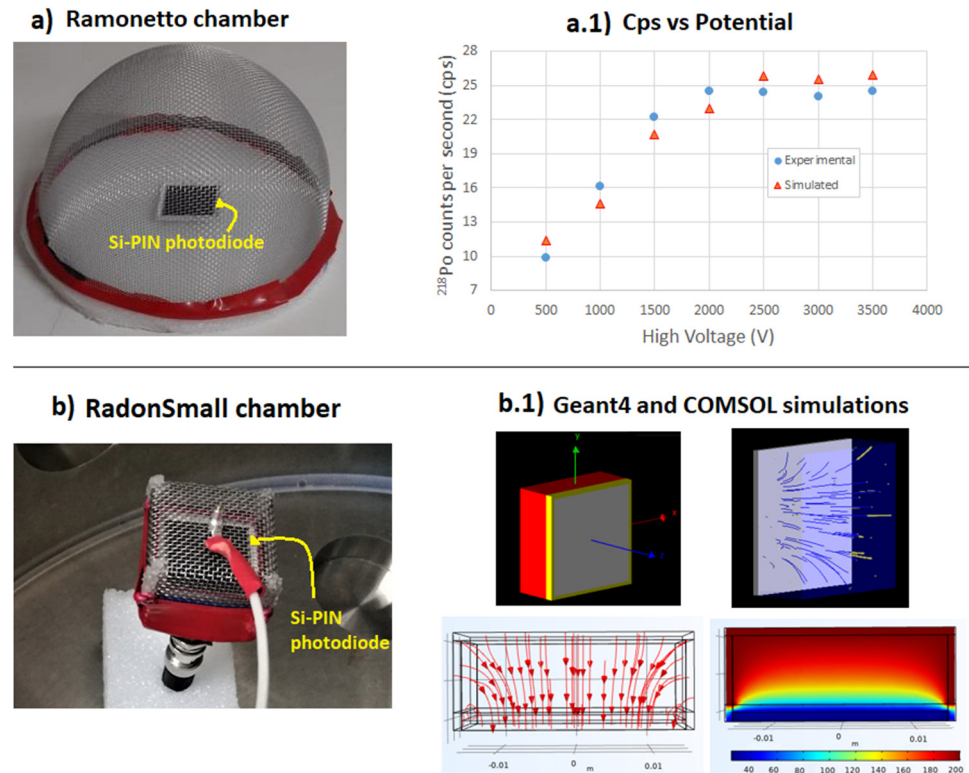


**Figure 3.** Ramonetto measurement chamber (a) and the graph of the experimental and simulated tests for choosing the best HV to apply (a.1). RadonSmall chamber, based on the prototype in [18] (b), with the correspondent Geant4+COMSOL simulations (b.1): Geant4 geometry and primary starting particles source (top), COMSOL electric potential and electric field (bottom).

Strengthened by all previous results, a final investigation has been conducted with the aim of simulating the detection efficiency of  $^{222-220}\text{Rn}$  and their progeny ( $^{218-216}\text{Po}$ ) versus different sizes of the three main geometries of the electrostatic collection measurements system (i.e., parallelepiped, cylinder and hemisphere), also varying the applied voltages. The silicon PIN photodiode of  $784 \pm 2 \text{ mm}^2$  square active area is fixed as detector in each simulation, always insulated in a plastic holder. Table 1 shows the obtained results. The main conclusions are: (i) detection efficiency is strongly dependent on the size of the chambers and on the voltage value applied to obtain electrostatic collection; (ii) detection efficiency decreases as chamber's height and/or radius increases, in agreement with the theoretical result that the detection efficiency of a radioactive source decrease as the distance source-detector increases; (iii)  $^{222-220}\text{Rn}$  efficiency depends on the height of the chambers due to the fact that both isotopes do not ionize, contrary to  $^{218-216}\text{Po}$  ions that are electrostatic collected, therefore, small chambers in height ensure the collection of the  $\alpha$ -particles of non-ionized  $^{220-222}\text{Rn}$  nuclei; (iv) the electric field inside the chamber is not strong enough to collect all the ions with low voltage value, while increasing the voltage the electric field intensifies and most of the ions are collected till the efficiency saturation is reached.



**Table 1.** Efficiency results of  $^{222-220}\text{Rn}$  and  $^{218-216}\text{Po}$  from the Geant4+COMSOL simulations of measurement systems based on electrostatic collection of  $\alpha$ -particles, by varying the size of the collection chambers and the high voltage applied to the metallic walls of the chambers.

Chamber (r = radius, h = height, s = side) [mm]	High Voltage [V] Uncertainty = $\pm 5$ V					$^{218-216}\text{Po}$ Efficiency [%] Mean Uncertainty = $\pm 2\%$					$^{222-220}\text{Rn}$ Efficiency (%) Mean Uncertainty = $\pm 2\%$				
Parallelepiped—h = 10, s = 28	70	120	200	350	500	26	30	31	32	31	23				
Parallelepiped—h = 40, s = 28	350	500	700	900	1000	16	19	23	24	24	7				
Hemisphere—h = 20, r = 20	50	100	200	350	500	18	25	30	35	35	28				
Hemisphere—h = 30, r = 30	100	200	400	600	800	13	18	23	27	27	13				
Cylinder—h = 10, r = 20	70	120	200	350	500	19	26	29	29	28	25				
Cylinder—h = 40, r = 20	350	700	800	950	1100	7	9	15	14	14	6				
High Voltage [V] Uncertainty = $\pm 5$ V	Chamber (r = radius, h = height, s = side) [mm]					$^{218-216}\text{Po}$ Efficiency [%] Mean Uncertainty = $\pm 2\%$					$^{222-220}\text{Rn}$ Efficiency (%) Mean Uncertainty = $\pm 2\%$				
350	Parallelepiped s = 28					47	43	26	21	13	44	37	14	9	6
	h = 1	h = 5	h = 20	h = 30	h = 45										
	Cylinder r = 20														
	h = 1	h = 5	h = 20	h = 30	h = 45										
	Cylinder h = 10														
500	r = 10	r = 15	r = 25	r = 30	r = 35	39	32	23	16	11	36	30	24	20	15
	Hemisphere														
500	r = 10	r = 15	r = 25	r = 35	r = 40	42	37	31	20	13	38	31	24	10	5

The overall results of the present work, prove the proper and correct working of the developed Geant4+COMSOL procedure in simulating measurement systems for the detection of  $^{222-220}\text{Rn}$  and their ionized progeny by electrostatic collection on a silicon detector, inside a metallic chamber.

### 5. Conclusions

The present paper provides, for the first time in literature, a useful tool to design and study, by simulation, the Radon and Thoron measurement systems based on the electrostatic collection of the  $\alpha$ -particle progeny. The proposed tool is a simulation procedure that uses a Monte Carlo method (Geant4) combined with a mathematical modeling software for solving partial differential equations (COMSOL) to recreate the entire process of Rn detection. Geant4 is for the interaction and transport of  $\alpha$ -particles through matter, while COMSOL determines the values of the electric fields applied to the collection chamber. To validate the tool, in this work we simulated worldwide commercial devices and compared our results with known experimental ones; then, we studied new measurement systems to optimize the chamber geometry and to obtain the best collection efficiency. The following achievements have been obtained: (1) the simulation tool gives results in agreement with those from the experiments, both in efficiency and in measurement spectrum; (2) based on the simulations, new devices were realized having efficiency greater than 20% and high counting rate for measuring directly Rn isotopes and their progeny; (3) a functional datasheet that compare the detection efficiency of  $^{222-220}\text{Rn}$  and their progeny ( $^{218-216}\text{Po}$ ), the different collection chamber geometries, and the dependence from the applied voltages.

**Author Contributions:** Conceptualization, F.A. and C.S.; methodology, F.A. and L.R.; software, F.A. and L.R.; validation, F.A., C.S. and V.R.; formal analysis, F.A. and L.R.; investigation, F.A., L.R., C.S., V.R. and A.D.; resources, F.A., C.S., V.R. and A.D.; data curation, F.A., L.R., C.S., V.R. and A.D.; writing—original draft preparation, F.A. and L.R.; writing—review and editing, F.A., L.R., C.S., V.R. and A.D.; visualization, F.A., C.S. and V.R.; supervision, F.A. and C.S.; project administration, F.A., C.S. and A. D.; funding acquisition, C.S., V.R. and A.D. All authors have read and agreed to the published version of the manuscript.

**Funding:** This research received no external funding.

**Institutional Review Board Statement:** Not applicable.

**Informed Consent Statement:** Not applicable.

**Data Availability Statement:** Not applicable.

**Conflicts of Interest:** The authors declare no conflict of interest.

## References

1. Siročić, A.P.; Stanko, D.; Sakač, N.; Dogančić, D.; Trojko, T. Short-term measurement of indoor radon concentration in northern Croatia. *Appl. Sci.* **2020**, *10*, 2341. [[CrossRef](#)]
2. Ambrosino, F.; Sabbarese, C.; Giudicepietro, F.; De Cesare, W.; Pugliese, M.; Roca, V. Study of surface emissions of  $^{220}\text{Rn}$  (thoron) at two sites in the Campi Flegrei caldera (Italy) during volcanic unrest in the period 2011–2017. *Appl. Sci.* **2021**, *11*, 5809. [[CrossRef](#)]
3. Woith, H. Radon earthquake precursor: A short review. *Eur. Phys. J. Spec. Top.* **2015**, *224*, 611–627. [[CrossRef](#)]
4. Ambrosino, F.; Sabbarese, C.; Roca, V.; Giudicepietro, F.; De Cesare, W. Connection between  $^{222}\text{Rn}$  emission and geophysical-geochemical parameters recorded during the volcanic unrest at Campi Flegrei caldera (2011–2017). *Appl. Radiat. Isot.* **2020**, *166*, 109385. [[CrossRef](#)] [[PubMed](#)]
5. Teterov, Y.G.; Tretyakova, S.P.; Golovchenko, A.N.; Ilić, R.; Skvarč, J. Determination of the absolute radon concentration in air using an electrostatic method and CR-39 detector. *Radiat. Meas.* **1995**, *25*, 645–646. [[CrossRef](#)]
6. Sabbarese, C.; Ambrosino, F.; Roca, V. Analysis by scanner of tracks produced by radon alpha particles in CR-39 detectors. *Radiat. Prot. Dosim.* **2020**, *191*, 154–159. [[CrossRef](#)]
7. Lane-Smith, D.; Sims, K.W.W. The effect of  $\text{CO}_2$  on the measurement of  $^{220}\text{Rn}$  and  $^{222}\text{Rn}$  with instruments utilising electrostatic precipitation. *Acta Geophys.* **2013**, *61*, 822–830. [[CrossRef](#)]
8. Salih, N.F.; Jafri, Z.M.; Aswood, M.S. Measurement of radon concentration in blood and urine samples collected from female cancer patients using RAD7. *J. Radiat. Res. Appl. Sci.* **2016**, *9*, 332–336. [[CrossRef](#)]
9. Ambrosino, F.; Sabbarese, C.; Roca, V.; Giudicepietro, F.; Chiodini, G. Analysis of 7-years Radon time series at Campi Flegrei area (Naples, Italy) using artificial neural network method. *Appl. Radiat. Isot.* **2020**, *163*, 109239. [[CrossRef](#)] [[PubMed](#)]
10. Theodoulou, G.; Parpottas, Y.; Tsertos, H. Systematic grid-wise radon concentration measurements and first radon map in Cyprus. *Radiat. Meas.* **2012**, *47*, 451–460. [[CrossRef](#)]
11. Sohrabi, M.; Ghahremani, M. Novel panorama megasize environmental radon monitor. *Radiat. Phys. Chem.* **2021**, *181*, 109325. [[CrossRef](#)]
12. Song, Y.; Shin, J.; Cho, S.; Yoo, S.; Cho, I.; Kim, E.; Jung, W.; Choi, S.; Oh, K. A comparison study of the ridge filter parameter by using FLUKA and GEANT4 simulation codes. *J. Korean Phys. Soc.* **2015**, *67*, 96–102. [[CrossRef](#)]
13. Pantelić, G.; Čeliković, I.; Živanović, M.; Vukanac, I.; Nikolić, J.K.; Cinelli, G.; Gruber, V. Qualitative overview of indoor radon surveys in Europe. *J. Environ. Radioact.* **2019**, *204*, 163–174. [[CrossRef](#)] [[PubMed](#)]
14. Ambrosino, F.; Thínová, L.; Briestenský, M.; Šebela, S.; Sabbarese, C. Detecting time series anomalies using hybrid methods applied to Radon signals recorded in caves for possible correlation with earthquakes. *Acta Geod. Geophys.* **2020**, *55*, 405–420. [[CrossRef](#)]
15. Nikolaev, V.A. Progress in the development of track radiometers for radon measurements. *Radiochemistry* **2019**, *61*, 396–407. [[CrossRef](#)]
16. Martín Sánchez, A.; dela Torre Pérez, J. Estimating retrospective indoor radon concentrations with a new device. *Appl. Radiat. Isot.* **2012**, *70*, 2742–2745. [[CrossRef](#)]
17. Alvarellós, A.; Chao, A.L.; Rabuñal, J.R.; García-Vidaurrázaga, M.D.; Pazos, A. Development of an automatic low-cost air quality control system: A radon application. *Appl. Sci.* **2021**, *11*, 2169. [[CrossRef](#)]
18. Sabot, B.; Pierre, S.; Michielsen, N.; Bondiguel, S.; Cassette, P. A new thoron atmosphere reference measurement system. *Appl. Radiat. Isot.* **2016**, *109*, 205–209. [[CrossRef](#)]
19. Ambrosino, F.; Sabbarese, C.; Buompane, R.; Roca, V. Development and calibration of a method for direct measurement of  $^{220}\text{Rn}$  (thoron) activity concentration. *Appl. Radiat. Isot.* **2020**, *166*, 109310. [[CrossRef](#)]
20. Barlas, E.; Bayrak, A.; Emirhan, E.; Haciomeroglu, S.; Ozben, C.S. Spatial distribution of  $^{214}\text{Po}$  ions in the electrostatic collection. *Appl. Radiat. Isot.* **2013**, *80*, 23–26. [[CrossRef](#)]
21. Bird, M.B.; Butler, S.L.; Hawkes, C.D.; Kotzer, T. Numerical modeling of fluid and electrical currents through geometries based on synchrotron X-ray tomographic images of reservoir rocks using Avizo and COMSOL. *Comput. Geosci.* **2014**, *73*, 6–16. [[CrossRef](#)]
22. Agostinelli, S.; Allison, J.; Amako, K.; Apostolakis, J.; Araujo, H.; Arce, P.; Asai, M.; Axen, D.; Banerjee, S.; Barrand, G.; et al. Geant4-a simulation toolkit. *Nucl. Instrum. Methods Phys. Res. A* **2003**, *506*, 250–303. [[CrossRef](#)]
23. Sabbarese, C.; Ambrosino, F.; Buompane, R.; Pugliese, M.; Roca, V. Analysis of alpha particles spectra of the Radon and Thoron progenies generated by an electrostatic collection detector using new software. *Appl. Radiat. Isot.* **2017**, *122*, 180–185. [[CrossRef](#)]
24. Hopke, P.K. The initial atmospheric behaviour of radon decay products. *J. Radioanal. Nucl. Chem.* **1996**, *203*, 353–375. [[CrossRef](#)]
25. Gu, S.; Ghosh, S. A finite element model for coupled 3D transient electromagnetic and structural dynamics problems. *Comput. Mech.* **2014**, *54*, 407–424. [[CrossRef](#)]
26. Tan, Y.; Xiao, D.; Tang, Q.; Shan, J.; Zhou, Q.; Liu, X. Research on the lower detection efficiency of the RAD7 for  $^{220}\text{Rn}$  than for  $^{222}\text{Rn}$ . *J. Instrum.* **2014**, *9*, T06001. [[CrossRef](#)]
27. Ambrosino, F.; Thínová, L.; Briestenský, M.; Giudicepietro, F.; Roca, V.; Sabbarese, C. Analysis of geophysical and meteorological parameters influencing  $^{222}\text{Rn}$  activity concentration in Mladeč caves (Czech Republic) and in soils of Phlegrean Fields caldera (Italy). *Appl. Radiat. Isot.* **2020**, *160*, 109140. [[CrossRef](#)]

28. Ambrosino, F.; Buompane, R.; Pugliese, M.; Roca, V.; Sabbarese, C. RaMonA system for radon and thoron measurement. *Nuovo Cimento C* **2018**, *41*, 222.
29. Berlier, F.; Cardellini, F.; Chiaberto, E.; Garlati, L.; Giuffrida, D.; Faure Ragani, M.; Leonardi, F.; Magnoni, M.; Minchillo, G.; Prandstatter, A.; et al. Main results of the second AIRP international radon-in-field intercomparison for passive measurement devices. *Radiat. Meas.* **2019**, *128*, 106177. [[CrossRef](#)]
30. Sabbarese, C.; Ambrosino, F.; D'Onofrio, A.; Roca, V. Radiological characterization of natural building materials from the Campania region (Southern Italy). *Constr. Build. Mater.* **2021**, *268*, 121087. [[CrossRef](#)]
31. Ambrosino, F.; Stellato, L.; Sabbarese, C. A case study on possible radiological contamination in the Lo Uttaro landfill site (Caserta, Italy). *J. Phys. Conf. Ser.* **2020**, *1548*, 012001. [[CrossRef](#)]
32. Bochicchio, F.; Campos-Venuti, G.; Piermattei, S.; Nuccetelli, C.; Risica, S.; Tommasino, L.; Torri, G.; Magnoni, M.; Agnesod, G.; Sgorbati, G.; et al. Annual average and seasonal variations of residential radon concentration for all the Italian Regions. *Radiat. Meas.* **2005**, *40*, 686–694. [[CrossRef](#)]
33. Sabbarese, C.; Ambrosino, F.; D'Onofrio, A.; Roca, V.; Pugliese, M. Natural radioactivity in soils and materials of the Campania region (Italy). *Nuovo Cimento C* **2020**, *43*, 152.